Seismic fragility curves for soft-storey buildings

Kittipoom Rodsin[1], Nelson Lam[1], John Wilson[2] and Helen Goldsworthy[1]

[1] The University of Melbourne
[2] Swinburne University of Technology

Abstract

Buildings with a soft-storey are notoriously vulnerable to collapse under strong earthquake shaking. However, a building subject to a small or moderate magnitude earthquake has a fair chance of survival depending on the drift demand on the soft-storey. This paper presents fragility curves which define the probability of collapse of a soft-storey column when subject to a pre-defined drift demand. The calculation for the fragility curves is based on the estimated shear (frictional) resistance to slip along a major diagonal shear crack (which is the plane of weakness for collapse to occur). The fragility curves presented can be shown to provide a more realistic representation of the seismic vulnerability of the building than the conventional approach based simply on the degradation in the horizontal resistance of the column.

Keywords: soft storey, collapse, fragility curves, column, seismic

1. Introduction

The research described in this paper forms part of a long-term program to assess and reduce the seismic risk and rationalizes the seismic design procedures and practices in Australia. Soft-storey buildings are considered to be particularly vulnerable because the rigid block at the upper levels has limited energy absorption and displacement capacity, thus leaving the columns in the soft-storey to deflect and absorb the inelastic energy. Collapse of the building is imminent when the energy absorption capacity or displacement capacity of the soft-storey columns is exceeded by the energy demand or the displacement demand.

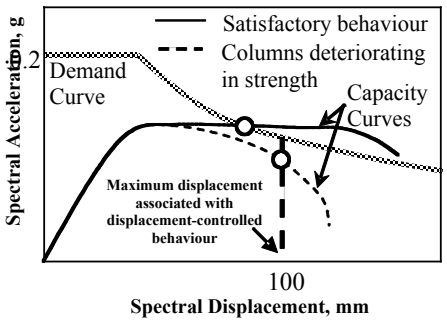

Figure 1 Schematic view of acceleration-displacement response spectrum diagram

This concept is illustrated using the 'Capacity Spectrum Method' shown in Figure 1 where the seismic demand is represented in the form of an acceleration-displacement response spectrum (ADRS diagram) and the structural capacity is estimated from a non-linear push-over analysis expressed in an acceleration-displacement relationship (as illustrated in Wilson & Lam 2003). The structure is considered to survive the design earthquake if the capacity curve intersects the demand curve and collapse if the curves do not intersect.

The current force-based design guidelines are founded on the concept of trading-off strength with ductility to ensure the structure has sufficient energy absorbing capacity. The limitation of this approach in lower seismic regions has been examined in Lam & Chandler (2005) in which the phenomenon of displacement-controlled behaviour was first introduced. By displacement-controlled behaviour, the peak displacement demand on the structure is well constrained around a definitive upper limit. Structures with seismic displacement capacity in excess of the seismic demand could be deemed seismically safe irrespective of the horizontal strength capacity or energy absorption capacity. Consequently, the authors have defined the ultimate drift capacity of a soft-storey building to be associated with the condition whereby the column can no longer resist gravity load. This definition is in contrast to the more conservative

approach used in high seismic regions where failure is deemed to occur when the lateral load resistance degrades by 20%.

The horizontal force-displacement behaviour of a soft-storey building can be modeled using classical approach of integrating curvature along the column. Contributions from deformation due to flexure, shear, yield penetration and joint rotation are then aggregated to calculate the horizontal displacement of the column. Pilot studies have been undertaken recently by the authors (Rodsin et al. 2004, 2005 and 2006) to predict displacement at the limit of collapse. For a column failing in flexure, collapse occurs soon after the rapid loss of the lateral strength capacity, in which case the displacement capacity at collapse could be predicted reasonably accurately using existing deformation models. In contrast, a column with widely spaced stirrups and with low aspect-ratios (hence failing in shear or flexure-shear) shows an early degradation in lateral strength. The rate of degradation is so gradual that a 2 - 3 % drift (at axial load ratio of approximately 0.2) could be sustained without the gravity load carrying capacity being compromised (Rodsin et al. 2004). This surprisingly high value of limiting drift is attributed partly to the widening of the major shear cracks. This additional drift capacity is given the notation: δ_{add}. Collapse is imminent when resistance to slip at one of the cracks has been exceeded.

This paper presents a new model for predicting the limiting drifts of non-ductile columns which pertain to fail in shear or flexure-shear due to their low aspect-ratios and wide stirrup spacings. The model is then extensively used to construct fragility curves based on the estimated shear resistance to slip along a major diagonal shear crack in Section 5.

2. Column shear failure

The ultimate behaviour of a column with low aspect-ratio and poor confinement is likely to be controlled by shear at the ultimate stage. The brittle shear failure (shear-dominated) of a column occurs before the flexural strength has been reached while ductile shear failure (flexural shear-dominated) occurs after plastic hinge in a column has been developed. The limit deformation at the onset of shear failure of a column failing in brittle shear could be accurately predicted once the column shear strength (V_{ini}) is known as shown in Figure 2 (curve 4).

For a ductile shear failure column, the shear strength of the column has been degraded as the ductility increases. The shear strength has degraded due to crushing of the compression strut of concrete in the compression zone and widening of the flexural shear crack which reduces the capacity of shear transfer by aggregate interlock. The well-known shear strength degradation as a function of ductility is shown in Figure 2.

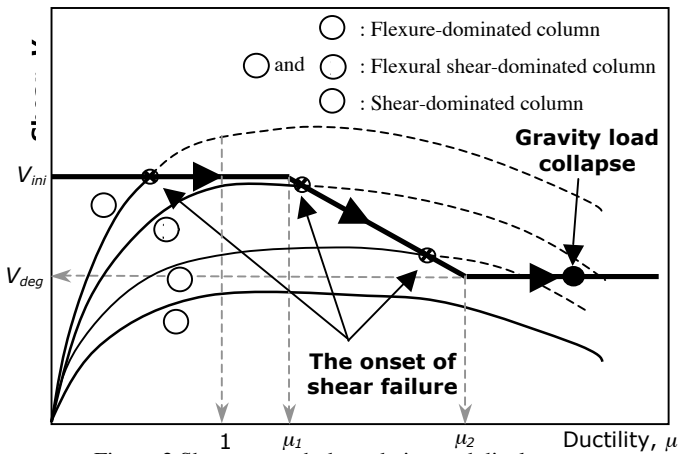

Figure 2 Shear strength degradation and displacement ductility

The onset of shear failure of a flexural shear-dominated column is predicted when degraded shear force capacity of the column intersects with the shear force demand as shown in curve 2 and 3. The "ductility dependent shear strength" relationships of columns have been proposed by many researchers (ie. Priestley et al. 1994 and Sezen & Moehle 2004).

Whilst the predicted shear strength V_{ini} using these models are agreed in general, these models provide significantly different results in predicting ductility dependent shear strength relationships. This is because the degraded concrete or the stirrup contributions to the total shear strength cannot be directly measured or defined from the test with

confidence (ie. the shear strength of a column cannot be measured when it does not fail in brittle shear). Consequently, the models developed empirically based on the test results provide only an approximate value which cannot be reliably used to estimate the degraded shear strength (V_{deg}) and the deformation at the onset of shear failure.

The model estimates degraded shear strength (V_{deg}) based on the equilibrium condition along the failure surface of a flexure-shear damage column has been developed by the authors and is presented in Section 3. In this study, the shear strength is assumed to linearly decrease with an increase in the displacement ductility. The values of μ_1 and μ_2 are conservatively assumed to be 2 and 3 respectively. The initial shear strength V_{ini} can be calculated using the predictive model suggested by ATC-40 1996.

The ductility dependent residual shear strength as shown in Figure 2 can be constructed when V_{ini}, V_{deg}, μ_1 and μ_2 are known. The onset of shear failure is predicted at the intersection between the degraded shear force capacity and demand as shown in Figure 2. The shear force demand relationship (inferred from the force-displacement relationship of the column) can be calculated using the deformation model proposed by Rodsin et al. (2005, 2006). From this force-displacement relationship, the yield displacement (δ_{yu}) which is corresponding to a ductility of one (μ = 1) can be determined by extrapolating the displacement at the first yield (δ_y) by the moment ratio (Priestley 1996) as shown in Equation 1.

$$\delta_{yu} = \frac{M_n}{M_y}\delta_y \qquad (1)$$

where M_n = the theoretical flexural strength of the column and M_y = the flexural strength corresponding to first yield of longitudinal bar.

At the onset of shear failure, the column may show some degradation of the lateral strength but without the axial load carrying capacity being compromised. It was observed from the recent experimental investigations that if no slippage occurs along the shear failure surface, then the column may rotate by a small angle α about the compression edge causing the crack to open slightly as shown in Figure 3a and increasing the lateral displacement capacity of the columns. This additional drift (δ_{add}) capacity after the onset of shear failure is of particular interest and is discussed further in Section 3. The total deformation at gravitational load collapse can be calculated from the summation of the deformation at the onset of shear failure and δ_{add}.

3. Limiting drift of a column failing in shear

The model presented herein is aimed at simplifying the mechanism of shear collapse in order that the column drift capacity (or limiting drift) could be conveniently estimated. The model for modeling collapse is shown schematically in Figure 3b. Collapse of the column is deemed imminent when the shear resistance along the crack interface (V_{ci}) (attributed to aggregate interlock) is exceeded by the shear force demand along the crack interface (V^*_{ci}). This shear force demand V^*_{ci} is often dominated by the axial load component resolved in the direction of slip. The procedure to calculate V^*_{ci}, V_{ci} and δ_{add} are presented in the following sections.

3.1 Calculation of shear force demand along the crack interface V^*_{ci}

The shear force applied along the crack interface V^*_{ci} can be calculated by equating the gravity load component and forces in the stirrups resolved in the direction along the shear failure surface as shown by Equation 2.

$$V^*_{ci} = P\cos\theta - F_{vy}\frac{h_c}{S}\cos\theta - F_{sc}\cos\theta + F_{st}\cos\theta + V_{deg}\sin\theta \qquad (2a)$$

where P = the gravity load; θ = the angle defining the orientation of the crack; F_{vy} = the stirrup yield strength; h_c is the width of the concrete core; and S = the stirrup spacing; F_{sc} = forces in the longitudinal reinforcement under compression F_{st} = forces in the longitudinal reinforcement under tension; and V_{deg} = the degraded shear force.

The angle θ can be estimated using the Modified Compression Field Theory (MCFT) or alternatively, a conservative value of 30 degree may be assumed for typical columns with shear span-to-depth ratio of between 2 and 3.

Forces in the longitudinal reinforcement under compression (F_{sc}) and tension (F_{st}) can be estimated using Equation 2 which is based on the assumption that the longitudinal reinforcements have buckled.

$$F_{sc} = 0.2 \cdot f_y A_{sc} \quad \text{and} \quad F_{st} = 0.2 \cdot f_y A_{st} \tag{2}$$

where f_y = the yield strength of the longitudinal reinforcement, A_{sc} = the total area of the longitudinal reinforcement under compression and A_{st} = the total area of the longitudinal reinforcement under tension.

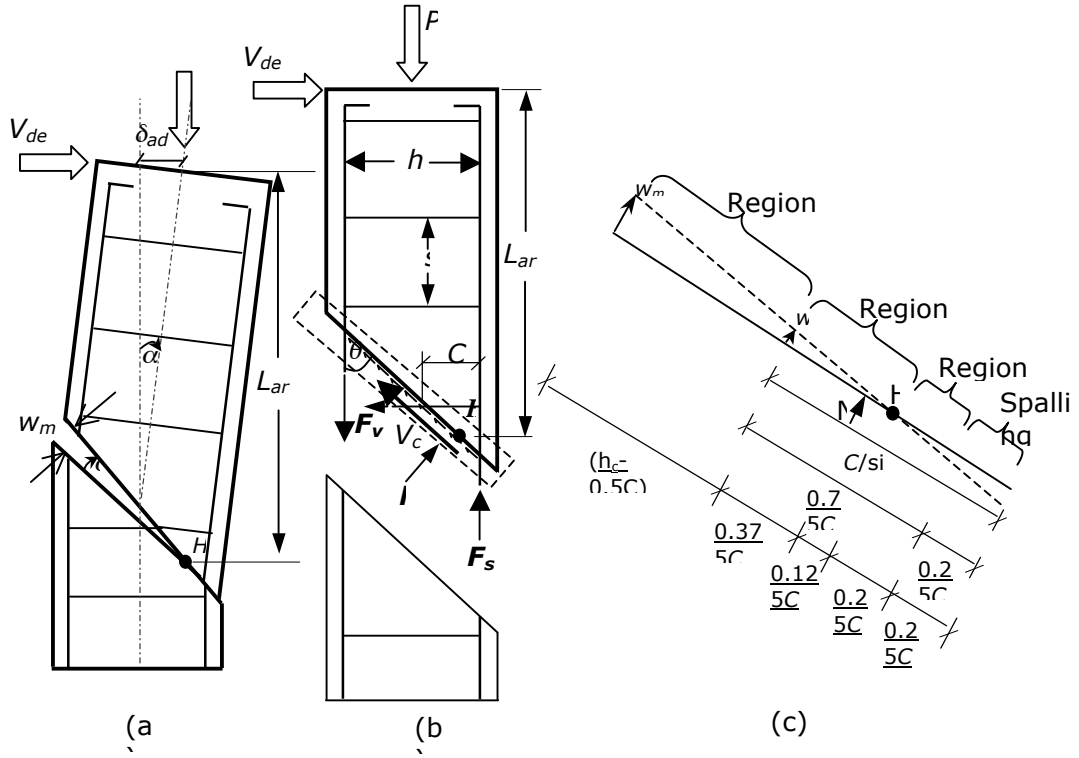

Figure 3 (a) additional displacement due to rotation at critical crack, (b) free body diagram of forces at the onset of shear failure and (c) geometry of the crack at the crack interface.

The unknown degraded shear strength (V_{deg}) and the force applied normal to the shear failure surface (N) can be calculated by solving Equations 3 and 4. Equation 3 is based on taking moment about point H (assumed to be at middle of the compression zone) as shown in Figure 3b. The assumption of plane strains remaining plane associated with bending deformation enables the depth of the compression block (C) (as shown in Figures 3b and 3c) to be estimated conveniently.

$$V_{\deg} = \frac{1}{L_{arm}}[0.5P \cdot (h_c - C) + F_{st} \cdot (h_c - 0.5C) + F_{sc} \cdot 0.5C - 0.125N \cdot \frac{C}{\sin\theta} + 0.5\frac{F_{vy} h_c}{\tan^2\theta \cdot S} \cdot (h_c - C)] \tag{3}$$

The equilibrium condition of forces in the direction normal to the shear failure surface is shown in Equation 4.

$$N = P\sin\theta + \frac{F_{vy}h_c}{S\tan\theta}\cdot\cos\theta + F_{st}\sin\theta - F_{sc}\sin\theta - V_{\deg}\cos\theta \quad (4)$$

3.2 Calculation of shear resistance of concrete along the crack interface V_{ci}

It is assumed that after the onset of shear failure shear forces are transferred across the crack only by aggregate interlock. The limit of shear force V_{ci} transferred by such a mechanism is a function of both crack width (w_{cr}) and the normal stress on the crack surface (σ). It is shown in Figure 4a that the crack width is not constant along the crack interface. Therefore, the crack interface is divided into 3 regions in order that the average normal stress and the average crack width in each region could be calculated and used to estimate shear resistance in regions I to III. The shear resistance V_{ci} from the 3 regions can be calculated using Equation 5.

$$V_{ci} = \sum_{n=I}^{n=III} v_{cin}A_{crn} = V_{ciI} + V_{cicII} + V_{cicIII} \quad (5)$$

where ν_{cin} = the shear stress transfer across the crack in region n; A_{crn} = the area of crack interface in region n; V_{ciI}, V_{ciII} and V_{ciIII} = the shear resistance in region I, II and III respectively.

The shear stress ν_{ci} in each region can be calculated in accordance with the relationship between shear transmitted across the crack, the normal stress on the crack and the crack width suggested by Vecchio & Collins (1986) as shown by Equations 6a and 6b.

$$v_{cin} = v_{ci\max n}\left(0.18 + 1.83\frac{\sigma_n}{v_{ci\max n}} - 1.01\left(\frac{\sigma_n}{v_{ci\max n}}\right)^2\right) \le v_{ci\max n} \quad (6a)$$

$$v_{ci\max n} = \frac{\sqrt{f_c'}}{0.3 + \frac{24w_{avgn}}{a+16}} \qquad \text{MPa, mm} \quad (6b)$$

where $\nu_{ci\ max\ n}$ = the maximum shear stress parameter in region n; σ_n = the normal stress on the shear failure surface in region n; w_{avgn} = the average crack width in region n.

3.3 Calculation of additional displacement δ_{add}

The average crack width in each region w_{avgI}, w_{avgII} and w_{avgIII} calculated based on the geometry of the crack (as shown in Figure 3c) is shown in Equation 7.

$$w_{avgI} = w_{\max}\frac{0.5h_c}{h_c - 0.5C},\ w_{avgII} = w_{\max}\frac{0.25C}{h_c - 0.5C} \text{ and } w_{avgIII} = 0 \quad (7)$$

In the model, it is assumed that the normal force N is applied to regions II and III and 25% of concrete in the compression zone has spalled as shown in Figure 3c. The normal stress in each region σI, σII and σIII can be calculated using Equation 8.

$$\sigma_I = 0,\quad \sigma_{II} = \frac{N\sin\theta}{0.75C\cdot b} \text{ and } \qquad \sigma_{III} = \sigma_{II} \quad (8)$$

where b = the width of the column section

The crack width w_{max} at axial load collapse can be obtained iteratively by matching value of V_{ci} (as calculated from Equations 5 – 8) with the value of V^*_{ci} (as calculated from Equation 2).

It was observed from recent experimental investigations by the authors that if slippage does not occur along the failure surface of the shear crack, then the part of the column

above the crack may rotate by a small angle α (which is approximately equivalent to additional drift) resulting in a small crack opening as shown in Figure 3a. The additional column deformation (δ_{add}) associated with this limiting crack opening can be calculated by substituting the maximum crack width w_{max} into Equations 9 and 10.

$$\alpha = \frac{w_{\max} \sin\theta}{h_c} \qquad (9) \qquad\qquad \delta_{add} = \alpha \cdot L_{arm} = w_{\max} \cdot \frac{\sin\theta}{h_c} L_{arm} \qquad (10)$$

where L_{arm} is the distance between the tip of the column and the rotation point H.

The calculated column deflection at the point of collapse may include the additional displacement δ_{add} associated with the limiting crack opening. It is noted that although the limiting angle of crack opening (α) at the threshold of collapse is generally very small, the associated increase in the displacement capacity of the column can be significant depending on the column geometry.

4. Experimental results

Half-scaled cantilever reinforced concrete column specimens with a similar cross-section of 160×200 mm and aspect ratios of 2.75 (S1) and 2.25 (S2) were tested to study their cyclic force-deformation behaviour under high shear force demand. The gravitational load carrying capacity of the column and mechanism of failure at collapse were studied. The innovative Vision Metrology System (VMS) was used to measure deformation of the columns including deformation of the area surrounding the shear cracks. The 3D displacement of the VMS targets attached to the surface of the columns was monitored throughout the test. Full details of the test can be found in Rodsin et al. (2004).

To validate the proposed model described in Section 3, data from the VMS targets located near the major shear crack have been analysed. The limiting angle of crack opening (α) and the additional displacement (δ_{add}) at the threshold of collapse were recorded for comparison with estimates obtained from the model (refer Table 1). The comparisons show general agreement between the experimental measurements and the analytical estimates. It should be noted that at this threshold of collapse, two displacement cycles have been applied to ascertain that the columns can sustain the cyclic loading without axial load carrying capacity being compromised.

Table 1 Comparison of experimental versus predicted crack rotation along the major crack plane, additional displacement (δ_{add}) and total displacement at incipient collapse.

Column	Length	Crack rotation (α)		Additional disp. (δ_{add})		Total disp. (δ)	
	mm	Radian (x10^{-3})		mm (%drift)		mm (%drift)	
		Exp.	Model	Exp.	Model	Exp.	Model
S1	550	5.8	6.6	2.9(0.5)	3.3(0.6)	21.0(3.8)	17.0(3.1)
S2	450	7.0	5.2	2.8(0.62)	2.1(0.47)	11.0(2.4)	9.3(2.1)

5. Fragility curve of soft-storey column failing in shear

The major uncertainties associated with additional displacement calculation are material properties, load conditions, the shear crack angle (θ) and the shear resistance along the crack surface. For the test column specimens, the first three parameters can be accurately measured with small variations so that they do not significantly affect the accuracy of the test results. In contrast, the mechanism of shear transfer across the crack is more complicated and the experimental data often show some degrees of scatter (as shown in Figure 4). Therefore, the fragility curves for a soft-storey column in this study are constructed based on the uncertainties associated with shear resistance to slip along a major diagonal shear crack. Fragility curves presented in this paper was based on laboratory controlled condition in which the values of ν_{cimax} and σ are predetermined.

These fragility curves could be further developed to incorporate variability in material properties, workmanship and load conditions encountered in practice.

The relationship between the measured shear stress transmitted across the crack and the compressive stress on the crack is shown in Figure 4. A non-linear regression analysis has been used to estimate the shear stress resistance ν_{ci} from Equation 6. The standard error (S.E.) was found to be 0.06. Although there is a limited number of data generated for each $\frac{\sigma}{v_{ci\max}}$, a considerable number of data covers a wide range of $\frac{\sigma}{v_{ci\max}}$ values. The statistical parameters in a regression analysis could be reliably estimated when there are sufficient data within the range of interest.

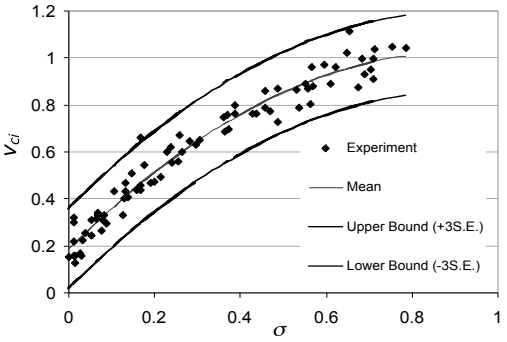

Figure 4 Relationships between normalized shear stress transmitted across crack (v_{ci}/v_{cimax}) and normalized compressive stress on crack (σ/v_{cimax}) (Vecchio and Collins, 1986).

A probability distribution of test data associated with crushing and spalling of materials usually follows a Gumbel distribution. However, under low $\frac{\sigma}{v_{ci\max}}$, only slippage along the crack interface (without material crushing) is expected. Therefore, a Gumbel distribution may not be applicable for modeling probability distribution for the whole range of data. For the sake of simplicity, it is assumed that the errors are normally distributed and there are about 2 chances in 3 that the data lies within the forecast equation (Equation 6) plus and minus one standard error. Therefore, the upper and lower bound (plus and minus 3 S.E.) plotted in Figure 4 show that there are 99.75% of data points lying within these two limits.

The fragility curve in Figure 5a is defined as a probability of gravity load collapse of shear damage columns when subject to a pre-defined additional displacement (δ_{add}) or a percentage drift. The probability of failure is calculated using a deterministic equation (Equation 6) to determine crack opening angle (α) (approximately equal to additional drift angle) at 50% chance of failure. A series of standard errors (S.E.) have been used to modify Equation 6 in order that other α values at a different probability of failure could be estimated. (ie. +1S.E. and -1S.E. associated with 83% and 17% probability of failure respectively).

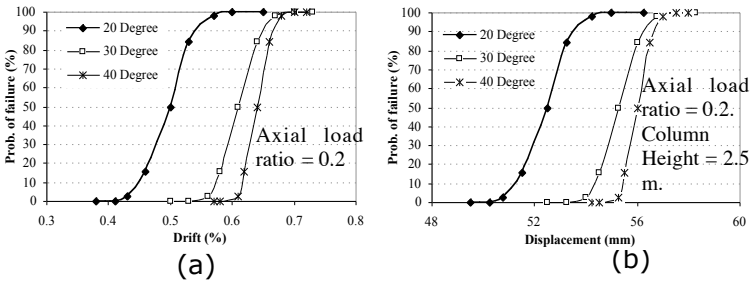

Figure 5 Fragility curves of (a) additional drift (crack opening angle) and (b) pre-defined displacement for different shear crack angles.

The fragility curves of a soft-storey building subject to a pre-defined displacement demand are shown in Figure 5b. To construct these fragility curves, the total drift is calculated by simply adding the drift at the onset of shear failure (the method of predicting drift at the onset of shear failure was suggested in Section 2) to the additional drift calculated in Figure 5a. This total drift is subsequently used to calculate the total displacement of a soft-storey column based on a given column height.

It was assumed that load conditions and geometry of an example column supporting soft-storey are similar to those of the column S2. The height of the first storey column is assumed to be 2.5 m (shear span = 1.25m). Therefore, the column specimen S2 was scaled from the corresponding prototype using a geometric scale factor of approximately 0.4 (0.45/1.25).

The displacement demand in Figure 5b is then presented in form of the peak ground velocity (PGV) as shown in Figures 6a-6c. The simplified response spectrum model for rock site in Australia as proposed by Wilson and Lam (2003) was used to estimate a displacement demand from a given PGV. Subsequently, the displacement demand was amplified using soil amplification factors S of 1.3, 1.8 and 3.0 for soil class B, C and D sites respectively. The corner period T2 is conservatively assumed to be 1.5 secs.

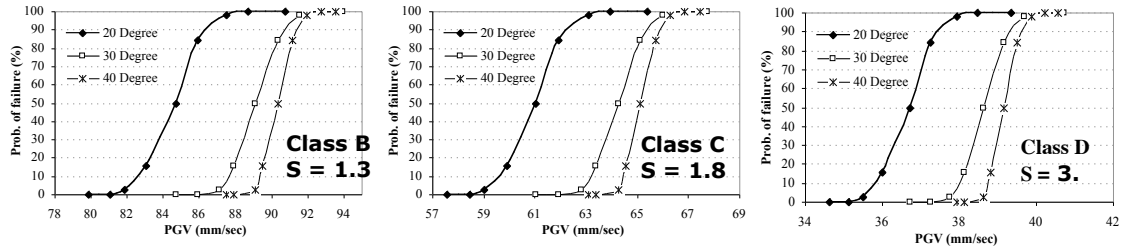

(a) (b) (c)

Figure 6 Fragility curves of a soft-storey column (the first storey height = 2.5m) for different shear crack angles under axial load ratio = 0.2.

From Figures 6a-6c, the soft-storey building founded on rock (class B) and shallow soil (class C) sites seems to be seismically safe (a notional PGV = 60 mm/sec). However, on the soft soil site (class D), this building may collapse when the PGV is greater than 40 mm/sec and is seismically safe when the PGV is lower than 35 mm/sec.

6. Conclusions

The concept of displacement-controlled behaviour has been introduced in this paper whereby the ultimate drift limit is based on the condition when gravity loading can no longer be supported by the damaged column. A model for predicting the deformation behaviour of a column at the limit of collapse has been presented. The model is intended for columns with low aspect-ratio and hence failing in shear or flexure-shear. The predictions calculated from the proposed models show good agreement with experimental results obtained from tests performed by the authors. The model has been further used to construct fragility curves which define the probability of collapse of a soft-storey column when subject to a pre-defined drift demand and a peak ground velocity based on different soil sites. The development of the gravity-collapse model for estimating the displacement capacity of soft-storey columns forms an important part of the displacement-based methodology for assessing the seismic performance of building structures in regions of low and moderate seismicity.

7. References

ATC40. 1996. Seismic evaluation and retrofitting of concrete buildings, Applied Technology Council, USA.

Lam, N.T.K. & Chandler, A.M. 2005. Peak displacement demand in stable continental regions, Earthquake Engineering and Structural Dynamics 34: 1047-1072.

Priestley, M.J.N., Verma, R. & Xiao, Y. 1995. Seismic shear strength of reinforced concrete columns, Journal of Structural Engineering 120(8): 2310-2329.

Rodsin, K., Lam, N.T.K., Wilson, J.L. & Goldsworthy, H. 2004. Shear controlled ultimate behaviour of non-ductile reinforced concrete columns, Procs. Conference of the Australian Earthquake Engineering Soc. 17. Mount Gambier: Australia.

Rodsin, K., Lam, N.T.K., Wilson, J.L. & Goldsworthy, H. 2005. Displacement limits for building collapse, Procs. Conference of the Australian Earthquake Engineering Soc. 33. Albury: Australia.

Rodsin, K., Lam, N.T.K., Wilson, J.L. & Goldsworthy, H. 2006. Collapse behaviour of columns with low aspect ratios, 19th Australasian Biennial Conference on the Mechanics of Structures and Materials, University of Canterbury, Christchurch, New Zealand to be published in 2006.

Sezen, H. & Moehle, J.P. 2004. Shear strength model for lightly reinforced concrete columns, Journal of Structural Engineering 130(11): 1692-1703.

Vecchio, F.J. & Collins, M. 1986. The modified compression field theory for reinforced concrete elements subjected to Shear, ACI Structural Journal 83(2): 219-231.